A NOVEL DESIGN OF SHORT-SEEKING CONTROL FOR DUAL-ACTUATOR HARD DISK DRIVES

Li Yang and Masayoshi Tomizuka

Department of Mechanical Engineering
University of California at Berkeley, Berkeley, California 94720, U.S.A.
yangli@me.berkeley.edu , *tomizuka@me.berkeley.edu*

Abstract: This paper discusses short seeking control for a dual-actuator hard disk drive consisting of a coarse actuator (voice coil motor, VCM) and a fine actuator (piezoelectric actuator, PZT). A novel design method is proposed based on the dual-stage track following control and initial value adjustment (IVA). This method, which adjusts the initial values of the track-following controllers for short seeking, makes the use of the feed-forward controller and reference trajectory unnecessary. The proposed design also takes into consideration the saturation property of the fine actuator by using a two-stage IVA scheme: (1) only VCM loop is utilized in the first stage (beyond PZT stroke limit), and IVA is designed to yield a high-speed seeking; (2) PZT loop is switched on when the read/write head approaches the target track in the second stage (within the PZT stroke limit), and IVA is used to produce a fast and smooth response. Simulation results verify the effectiveness of the proposed method.

Keywords: dual actuator, short seeking, actuator saturation, hard disk drives (HDDs)

1. INTRODUCTION

The hard disk drive industry continues to strive for increased storage densities and reduced data access times. This demands performance improvements of the head positioning system in terms of fast track seeking and precise track following of the target track. To meet these requirements, the servo bandwidth of the head positioning system must be increased to reject a wider range of disturbances such as disk flutter vibrations, spindle run-out, windage, and external vibration. The servo bandwidth, however, is mainly limited by the actuator's mechanical resonance modes. Dual-stage actuation has been recognized as a powerful candidate to expand the servo bandwidth. The dual-actuator disk file system consists of two actuators: coarse and fine actuators. The coarse actuator is of low bandwidth with a large operating range and it is used for coarse positioning; the voice coil motor (VCM) is the most popular coarse actuator. The fine actuator is of high bandwidth with a small operating range and it is used for fine positioning; the piezoelectric transducer (PZT) is a popular fine actuator.

The dual-stage actuator can improve both track-following and track-seeking performance. Many research efforts have been devoted to the design of the track following servo using dual-stage actuators. Several designs for dual stage track-following servos have been proposed, such as a parallel type (Ding, *et al.*, 2000; Semba, *et al.*, 1999), a decoupled type (Mori, *et al.*, 1991), a master-slave type (Koganezawa, *et al.*, 1999), and a u-synthesis MIMO type (Hernandez, *et al.*, 1999). However, short seeking performance of dual-stage servos has not been discussed much. It has only been evaluated based on step responses of a closed-loop track-following feedback system, or alternatively, achieved by a two-degree-of-freedom (TDOF) servo structure, which requires the design and implementation of both the feed-forward controller and reference trajectory (Kobayashi and Horowitz, 2001; Ding, *et al.*, 2004).

In this paper, we propose a novel method for dual stage short seeking control based on dual-stage track following control and initial value adjustment. This method, which utilizes the same controllers as in track following, tunes the initial values of track-

following controllers for short seeking. By tuning the initial values of the feedback controller, the desired transient characteristics in short-seeking can be obtained without the use of feed-forward controller and reference trajectory, which implies no real time computation for feed-forward control is needed. As the fine PZT actuator has a stroke limit of only a few micrometers, the design for the short seeking also take into consideration the saturation properties of the PZT actuator. When the short-seek distance is over PZT stroke limit, a two-stage IVA scheme is designed in such a way that only VCM loop is utilized in the first stage (beyond PZT stroke limit), and the PZT loop are switched on when the read/write head approaches the target track in the second stage (within the PZT stroke limit). The first stage IVA is designed to yield a high-speed seeking, and the second stage IVA is used to produce a fast and smooth response as the output approaches the command input.

The remainder of this paper is organized as follows. Section 2 describes the structure of a dual-actuator HDD and the track-following controller design. Section 3 presents the proposed dual-stage short seeking control with IVA. Both one-track seek design and short-span seeking (over PZT stroke limit) design are discussed along with the simulation results. Conclusions are given in Section 4.

2. DUAL ACTUATOR SYSTEM AND TRACK FOLLOWING CONTROLLER DESIGN

Fig. 1 shows the HDD with VCM as a first actuator and a PZT as a secondary actuator. PZT stroke limit is $\pm 1.0um$. The actual HDD was modeled through frequency response test and Fig. 2 shows the frequency responses of VCM and PZT plant models. Notice that the VCM pant model has double integrators with three resonance modes and PZT pant model has three resonances at high frequencies.

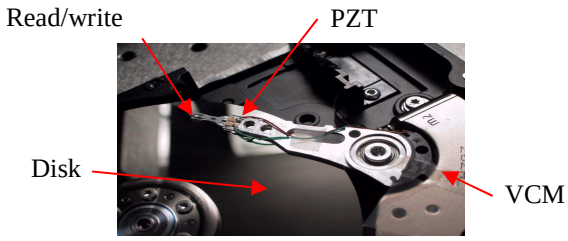

Fig. 1 Dual-actuator Hard Disk Drive

In this study, the parallel track-following servo controller is used to achieve high-accuracy track following (Ding, *et al*., 2000). The servo structure is shown in Fig.3. P_{VCM} and P_{PZT} represent the plant models of VCM and PZT, respectively. C_1 and C_2 are, respectively, controllers for the VCM and PZT actuators. The VCM controller is designed to stabilize the VCM loop for preventing damage to disk drive systems when the PZT is not activated, and achieve basic performance. It is designed to be a phase-lag-lead compensator. The PZT controller is designed to achieve overall performance and is a phase-lag compensator with two notch filters.

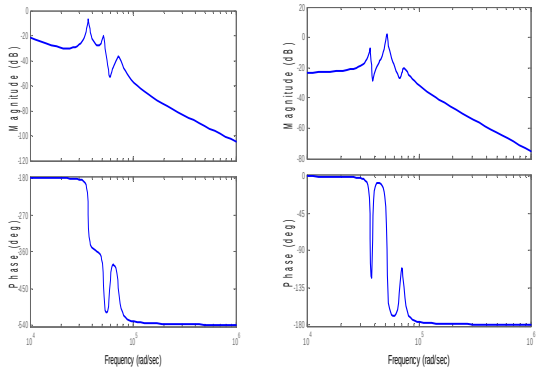

Fig. 2 Frequency responses of VCM and PZT plants

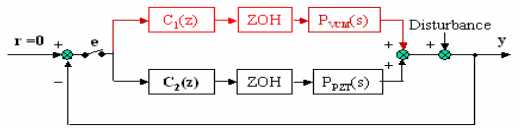

Fig 3 Tracking following control system for dual-actuator HDDs

3. DUAL STAGE SHORT SEEKING CONTROL WITH INITIAL VALUE ADJUSTMENT

In this section, we will discuss short seeking control with IVA for the dual-actuator HDDs. We first explain one-track seeking design and then discuss the short-span seeking (over PZT stroke limit) design.

3.1 One-Track Seeking Design

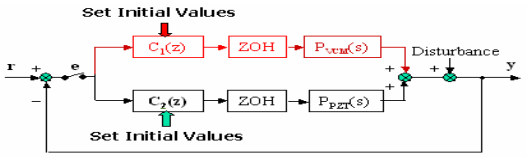

Fig. 4 1-track seek with IVA for dual-actuator HDDs

Fig. 4 shows a schematic diagram of 1-track seeking control with IVA for dual-actuator HDDs. The proposed method has the following features:

(1) The overall structure during seeking is a one-degree-of-freedom structure.
(2) Reference input is set to be a step signal, i.e., $r(k)=r$ for $k \geq 0$, where r is the seeking distance. Output y is the head position, which can be measured. The feedback controllers are the same as the dual-stage track following controllers.
(3) Nonzero initial values are set to both controllers for 1-track seeking.

Notice that the adjustment of the initial values of the controller improves the transient response without changing closed-loop characteristics such as stability and sensitivity. Since we already have the track following controllers, finding the initial values

of the controllers becomes the main issue. In the following sub-section *3.1.1*, the closed loop system depicted in Fig. 4 is represented in time domain. Then in sub-section *3.1.2*, IVA of the controllers is formulated as an optimization problem by finding the optimal initial states of the controllers to minimize the performance index based on the tracking error. Design of performance index for short-seeking is discussed in sub-section *3.1.3*. Simulation results are given in Sub-section *3.1.4*.

3.1.1 Close loop system in time domain

Assume that the dynamic models of VCM plant and PZT plant in continuous time are

$$\begin{aligned} \dot{x}_v(t) &= A_{01}x_v(t) + B_{01}u_v(t) \\ y_v(t) &= C_{01}x_v(t) \end{aligned} \quad (1)$$

and

$$\begin{aligned} \dot{x}_p(t) &= A_{02}x_p(t) + B_{02}u_p(t) \\ y_p(t) &= C_{02}x_p(t) \end{aligned} \quad (2)$$

where $x_v \in \Re^{n_v}$, u_v and y_v are the state vector, control input and output of VCM, and $x_p \in \Re^{n_p}$, u_p, y_p are the state vector, control input and output of PZT.
The discrete time equivalents of (1) and (2) with sampling period *Ts* can be expressed by

$$\begin{aligned} x_v(k+1) &= A_v x_v(k) + B_v u_v(k) \\ y_v(k) &= C_v x_v(k) \end{aligned} \quad (3)$$

and

$$\begin{aligned} x_p(k+1) &= A_p x_p(k) + B_p u_p(k) \\ y_p(k) &= C_p x_p(k) \end{aligned} \quad (4)$$

where $A_v \in \Re^{n_v^2}, B_v \in \Re^{n_v}, C_v \in \Re^{1\times n_v}$,

$A_p \in \Re^{n_p^2}, B_p \in \Re^{n_p}, C_p \in \Re^{1\times n_p}$

Suppose VCM controller and PZT controller $C_1(z)$, C_2 (z) can be expressed in time domain as follows:

$$\begin{aligned} x_{vc}(k+1) &= A_{vc}x_{vc}(k) + B_{vc}e(k) \\ u_v(k) &= C_{vc}x_{vc}(k) + D_{vc}e(k) \end{aligned} \quad (5)$$

and

$$\begin{aligned} x_{pc}(k+1) &= A_{pc}x_{pc}(k) + B_{pc}e(k) \\ u_p(k) &= C_{pc}x_{pc}(k) + D_{pc}e(k) \end{aligned} \quad (6)$$

where $x_{vc} \in \Re^{n_{vc}}$, $A_{vc} \in \Re^{n_{vc}^2}, B_{vc} \in \Re^{n_{vc}}, C_{vc} \in \Re^{1\times n_{vc}}, D_{vc} \in \Re$

$x_{pc} \in \Re^{n_{pc}}$, $A_{pc} \in \Re^{n_{pc}^2}, B_{pc} \in \Re^{n_{pc}}, C_{pc} \in \Re^{1\times n_{pc}}, D_{pc} \in \Re$.

Combining the controllers equations (5), (6) and plants equations (3), (4) and referring to Fig. 4, we can obtain the closed loop system:

$$\begin{aligned} x(k+1) &= Ax(k) + B\,r \\ y(k) &= Cx(k) + D\,r \end{aligned} \quad (7)$$

where $x(k) := [x_v(k)^T, x_p(k)^T, x_{vc}(k)^T, x_{pc}(k)^T]^T \in \Re^{n_v+n_p+n_{vc}+n_{pc}}$

Matrices *A, B, C, D* can be computed from the system matrices in (3)~(6). Notice that the states of the closed loop system $x(k)$ can be separated into two parts: the states of two plants ($x_k(k)$) and the states of two controllers ($x_c(k)$):

$$x_k(k) := \begin{bmatrix} x_v(k) \\ x_p(k) \end{bmatrix}, \quad x_c(k) := \begin{bmatrix} x_{vc}(k) \\ x_{pc}(k) \end{bmatrix}.$$

The resulting closed loop system (7) is asymptotically stable because the track following controller has been designed to stabilize the system. The error dynamics of the closed loop system is:

$$e_x(k+1) = Ae_x(k) \quad (8)$$

where $e_x(k) = x(k) - x(\infty), \quad x(\infty) = (I-A)^{-1}Br$ (9)

3.1.2 Initial Value Adjustment of the Controllers

Now the initial value adjustment of the controller can be formulated as the following optimization problem.
Problem: Consider the control system descried by equation (7). Find the initial value of the controller $x_c(0)$ that minimizes performance index *J:*

$$J = \sum_{k=0}^{\infty} e_x(k)^T Q\, e_x(k), \quad for\, Q > 0 \quad (10)$$

where $e_x(k)$ is as defined in (9).

Theorem 1: The initial value of the controller $x_c(0)$ that minimizes performance index *J* is:

$$x_c(0) = K_1 r + K_2 x_k(0) \quad (11)$$

where $K_1 = [P_{22}^{-1}P_{12}^T \quad I](I-A)^{-1}B, \quad K_2 = -P_{22}^{-1}P_{12}^T$ (12)

and P_{22}, P_{12} are obtained by the Lyapunov Eq.:

$$A^T PA - P = -Q, \quad P =: \begin{bmatrix} P_{11} & P_{12} \\ P_{12}^T & P_{22} \end{bmatrix} \quad (13)$$

Proof: Since *A* is asymptotically stable, (13) has a unique positive definite solution P>0, and *J* can be transformed to:

$$J = e_x(0)^T P\, e_x(0)$$

where

$$e_x(0) = x(0) - x(\infty) = \begin{bmatrix} x_k(0) \\ x_c(0) \end{bmatrix} - x(\infty) =: \begin{bmatrix} e_k(0) \\ e_c(0) \end{bmatrix} \quad (14)$$

So, $J = e_k^T(0)P_{11}e_k(0) + 2e_k^T(0)P_{12}e_c(0) + e_c^T(0)P_{22}e_c(0)$
It is easy to show that $\partial J/\partial x_c(0) = 0$ is equivalent to $\partial J/\partial e_c(0) = 0$. Solving $\partial J/\partial e_c(0) = 0$, we get

$$e_c(0) = -P_{22}^{-1}P_{12}^T e_k(0) \quad (16)$$

From (14), (16) and (9), we conclude that J is minimized for $x_c(0) = K_1 r + K_2 x_k(0)$, where K_1, K_2 are as defined in (12). □

Noting that $x_k(0)$ may be assumed zero for 1-track seek, the initial value of the controllers turned out to be a simple form as:

$$x_c(0) = K_1 r, \quad K_1 = [P_{22}^{-1}P_{12}^T \quad I](I-A)^{-1}B \quad (17)$$

3.1.3 Design of Performance Index Function

The performance index *J* plays an important role in determining the initial value of the controller and thus the short seeking performance.

Design I- considering tracking error at sampling points

It is straightforward to evaluate the tracking error at sampling points and consider smoothness of the

output and control input in the performance index as:

$$J = \sum_{k=0}^{\infty} [e_y(k)^2 + q_1 \dot{e}_y(k)^2] + q_2 J_u \qquad (18)$$

where $e_y(k) = y(k) - y(\infty)$, $\dot{e}_y(k) := [e_y(k+1) - e_y(k)]/T_s$

$$J_u = \sum_{k=0}^{\infty} [U(k) - U(\infty)]^T [U(k) - U(\infty)], \quad U(k) = [u_v(k), \ u_p(k)]^T \qquad (19)$$

and q_1, q_2 are weighting factors.

Lemma 1: The performance index J in (18) can be transformed into the standard quadratic form:

$$J = \sum_{k=0}^{\infty} e_x(k)^T Q \, e_x(k)$$

where $Q = C^T C + q_1 C_d{}^T C_d + q_2 C_u{}^T C_u$,

$$C_d = C\frac{A - I}{T_s}, \ C_u = \begin{bmatrix} -D_{vc}C_v, -D_{vc}C_p, C_{vc}, \ O \\ -D_{pc}C_v, -D_{pc}C_p, O, C_{pc} \end{bmatrix} \qquad (20)$$

The proof is omitted due to the space limitation.

Design II- considering the inter-sampling behaviors

Design method I only evaluates the tracking error at the sampling instants. However, the plant is a continuous-time system, and it is natural to evaluate the continuous-time signals directly. Especially in dual-stage servos, inter-sampling ripple may take place if the second actuator has mechanical resonance modes at high frequencies beyond sampling frequency, which can be excited by the control input. To incorporate the inter-sampling error, we modify J in (18) as follows:

$$J = \int_0^{\infty} [e_y(t)^2 + q_1 \dot{e}_y(t)^2] dt + q_2 J_u \qquad (23)$$

where $e_y(t) = y(t) - y(\infty)$, J_u is as defined in (19).

To evaluate (23), the pieces of the continuous-time state $x_k(t)$ and $e_k(t)$ are introduced as:

$$\begin{aligned} x_k(k)(v) &= x_k(kT_s + v) \\ e_k(k)(v) &= e_k(kT_s + v) \end{aligned}, \quad v \in [0, T_s) \qquad (24)$$

where $e_x(t) = x(t) - x(\infty) = [e_k(t)^T, e_c(t)^T]^T$

Lemma 2: $e_k(k)(v)$ is a function of error-vector $e_x(k)$:

$$e_k(k)(v) = He^{\hat{A}v} \bar{S} e_x(k), \ v \in [0, T_s] \qquad (25)$$

where

$$\hat{A} = \begin{bmatrix} \hat{A}_{01} & O \\ O & \hat{A}_{02} \end{bmatrix}, \hat{A}_{01} = \begin{bmatrix} A_{01} & B_{01} \\ O & O \end{bmatrix}, \hat{A}_{02} = \begin{bmatrix} A_{02} & B_{02} \\ O & O \end{bmatrix}$$

$$\bar{S} = \begin{bmatrix} S_v \\ S_p \end{bmatrix} \times \begin{bmatrix} I_{n_v}, O \\ O_{n_p \times n_v}, I_{n_p}, O_{n_p \times (n_{vc} + n_{pc})} \\ C_u \end{bmatrix}, H = \begin{bmatrix} [I_{n_v}, O], \ O \\ O, \ [I_{n_p}, O] \end{bmatrix}$$

$$S_v = \begin{bmatrix} I_{n_v}, \ O_{n_v \times (n_p + 2)} \\ 0, ..., 0, \ 1, \ 0 \end{bmatrix}, S_p = \begin{bmatrix} O_{n_p \times n_v}, I_{n_p}, O_{n_p \times 2} \\ 0, ..., 0, \ \ 0, \ \ 1 \end{bmatrix}$$

The proof is omitted due to the space limitation.

Noting that

$$\begin{aligned} y(k)(v) &= y_v(k)(v) + y_p(k)(v) = C_{01}x_v(k)(v) + C_{02}x_p(k)(v) \\ &= \hat{C}_0 x_k(k)(v), \ \ \hat{C}_0 = [C_{01} \ \ C_{02}], \\ y(k)(v) - y(\infty) &= \hat{C}_0 e_k(k)(v) \end{aligned} \qquad (26)$$

and using Lemma 3 , we obtain

$$\begin{aligned} J_1 &= \int_0^{\infty} e_y(t)^2 dt = \sum_{k=0}^{\infty} \{ \int_0^{T_s} [y(k)(v) - y(\infty)] dv \} \\ &= \sum_{k=0}^{\infty} \{ \int_0^{T_s} e_k^T(k)(v) Q_{cc} e_k(k)(v) dv \} \\ &= \sum_{k=0}^{\infty} \{ e_x^T(k) \bar{S}^T (\int_0^{T_s} e^{\hat{A}^T v} (H^T Q_{cc} H) e^{\hat{A} v} dv) \bar{S} e_x(k) \} \\ &= \sum_{k=0}^{\infty} \{ e_x^T(k) \bar{S}^T \hat{Q}_c \bar{S} e_x(k) \} = \sum_{k=0}^{\infty} e_x(k)^T Q_1 e_x(k) \end{aligned}$$

where $Q_1 = \bar{S}^T \hat{Q}_c \bar{S}$, $\hat{Q}_c = \int_0^{T_s} e^{\hat{A}^T v} (H^T Q_{cc} H) e^{\hat{A} v} dv$, $Q_{cc} = \hat{C}_0^T \hat{C}_0$

Thus, we conclude that the performance index J in (23) can also be transformed into the standard quadratic form as: $J = \sum_{k=0}^{\infty} e_x(k)^T Q \, e_x(k)$.

3.1.4 One-track Seeking Simulations

We used the same plant models (as in fig. 2) and track-following controllers as discussed in Section 2, and assumed a density of 25.4 kTPI (one-track pitch is 1 *um*) for the simulations. Fig. 5 shows the response of the output without initial value adjustment of the controllers for 1-track seeking. The dark line shows the head position, the light line and dotted line are VCM and PZT position respectively. Simulation results of 1-track seeking using proposed method are shown in Fig. 6. From Fig. 6, we can see that a fast and smooth response in short seeking can be achieved by IVA of the controllers. The design parameters q_1, q_2 are set as follows after some trial and errors: q_1*=0.09*, q_2*=0.005*. And initial values of the controllers are calculated by (17).

It could be noted from Fig. 6 that the dual-stage seeking control greatly improves the responses. It takes about 0.3 ms to move the head to the desired track so that the head can read or write data on the data track. The PZT actuator first moves towards the target track, and then returns to its stroke center to cancel out the movement of the VCM actuator after the head is on track. We can see PZT is within its stroke limit. Fig 6 (c) compares the performance of *Design I* and *Design II*, which confirms that inter-sampling ripple is decreased using *Design II*.

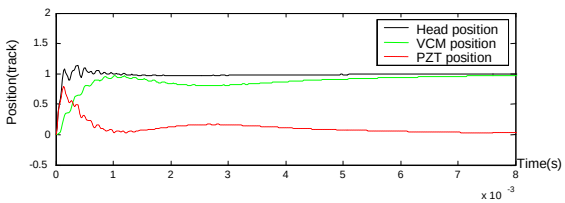

Fig. 5 1-track seek without IVA for dual-actuator HDD

From Eq. (17), we can see the initial values of the controllers are scaled with seeking distance r, so are the responses of both actuators. As seeking distance becomes longer, the PZT response will exceed its stroke limit as the upper figure of Fig 7, where r=3. If the saturation property is considered, the performance is degraded as the lower figure of Fig.

7. In the next section, we will discuss the short-span seeking when the head moves over the PZT actuator's stroke limit.

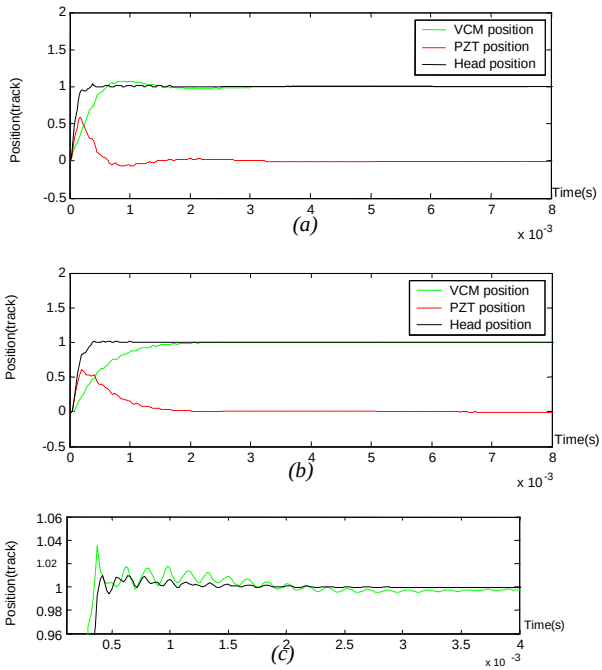

Fig. 6 1-track seek with IVA for dual-actuator HDDs:(a) *Design I;* (b) *Design II*; (c) Head position around target track, dark line: *Design II*; light line: *Design I.*

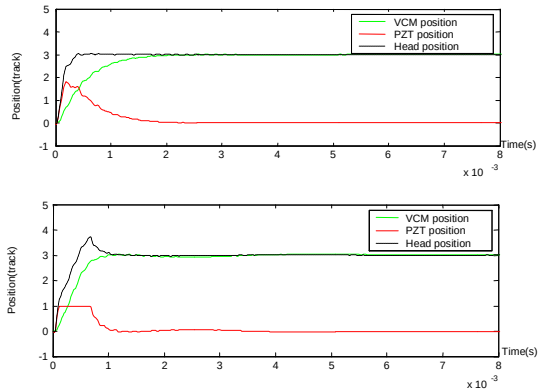

Fig. 7 3-um seek using IVA (Response Over PZT Stroke Limit)

3.2 Short-span Seeking (Over PZT Stroke Limit)

3.2.1 Overall Control Structure for Short Seeking

Fig. 8 and 9 show the schematic diagrams of short seeking control with IVA for dual-actuator HDDs, where the seeking distance is over PZT stroke limit. The proposed method has the following features:

(1) The overall short-span seeking is divided into two stages, as referred to Fig. 9: in the first stage, where the head is beyond the PZT operation range, only VCM actuator and its controller is used; in the second stage, where the head is approaching the target track (within the PZT operation range), the PZT actuator and its controller are switched on.

(2) Reference input is set to be a step signal for the whole short-span seeking, i.e., $r(k)=r$ for $k \geq 0$, where r is the seeking distance. The feedback controllers are the same as the dual-stage track following controllers.

(3) Nonzero initial values are set to the corresponding controller (controllers) at the start instant of each stage to achieve desired short seek performance.

For simplicity, we will explain in two-stage design procedure.

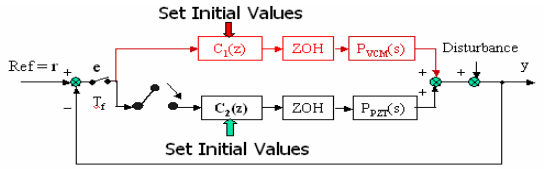

Fig.8 Dual-stage Short-seek control with IVA considering PZT actuator saturation

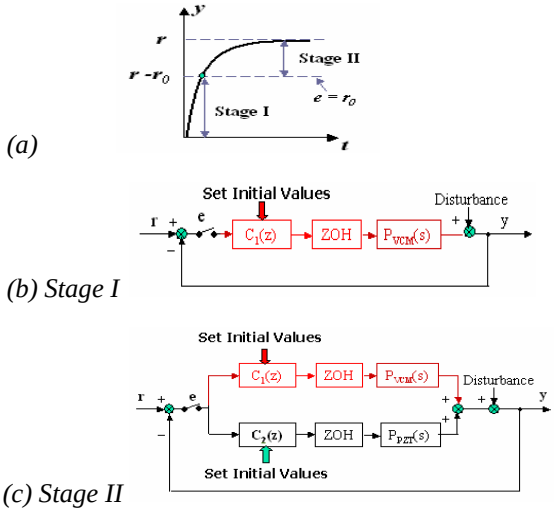

Fig.9 Dual-stage short-seek with two-stage IVA

3.2.2 Stage-I Design ($e > r_0$)

In the first stage we use the servo system shown as Fig. 9 (b), which involves only VCM loop. The initial value of C_1 can be obtained following the same procedure as Section 3.1 by first obtaining the closed loop system depicted in Fig.9 (b) in time domain as:

$$\begin{aligned} x(k+1) &= Ax(k) + B\,r \\ y(k) &= Cx(k) + D\,r \end{aligned} \tag{27}$$

where

$$x(k) \coloneqq \begin{bmatrix} x_v(k) \\ x_{vc}(k) \end{bmatrix},\ A = \begin{Bmatrix} \begin{bmatrix} A_v & B_v C_{vc} \\ 0 & A_{vc} \end{bmatrix} - \begin{bmatrix} B_v D_{vc} \\ B_{vc} \end{bmatrix} \begin{bmatrix} C_v & O \end{bmatrix} \end{Bmatrix},\ B = \begin{bmatrix} B_v D_{vc} \\ B_{vc} \end{bmatrix}$$

$$C = \begin{bmatrix} C_v & O \end{bmatrix},\ D = O \tag{28}$$

The initial value of controller C_1 can be obtained using Theorem 1 as: $x_{vc}(0) = K_1 r$

where $K_1 = [P_{22}^{-1} P_{12}^{T}, I](I-A)^{-1}B$, and P_{22}, P_{12} are obtained by solving the Lyapunov equation:

$A^T P A - P = -Q$, $P \coloneqq \begin{bmatrix} P_{11} & P_{12} \\ P_{12}^T & P_{22} \end{bmatrix}$, A is as defined in (28)

The objective of IVA in the *Stage I* is to get a rapid response, so we design the performance index only based on the tracking error ignoring the smoothness terms as: $J = \sum_{k=0}^{\infty} e_y(k)^2$, and so $Q=C^TC$ by Lemma 1, where C is defined in (28).

3.2.3 Stage-II Design ($e \le r_0$)

The PZT loop is activated at the instance $e=r_0$, and in stage-*II*, we use the servo system in Fig. 9 (c), which is the same as that of 1-track seeking, except that the initial value of the plants $x_k(0)$ is not zero here. Nonzero initial values are set to the controllers at the switching instance. The initial value here refers to the state at the switching instance. The initial values of $C_1$and C_2 can be obtained following the same procedure as 1-track seeking by first obtaining the closed loop system in Fig.9 (c) as (7), and then finding the optimal initial values of the controller using Theorem 1. Notice that the initial values of the controllers are determined by (11) instead of (17), due to the nonzero initial values of the plants. The objective of IVA in *Stage II* is to get a fast and smooth response as the output approaches the target, and performance index is designed using *Design method I* as (18*), or* using *Design method II* as (23) for enhanced inter-sampling performance.

3.2.4 Short-span Seeking Simulations

Now, we evaluated *3-um* seeking responses, which are over the PZT actuator stroke limit. Simulation results of 3-*um* seeking using proposed method are shown in Fig. 10. Here *r= 3* and we set r_0 to be 2. We can see that a fast and smooth response in short seeking can be achieved. Compared with Fig.10 (a), Fig.10 (b) shows that inter-sampling performance is improved using *Design II*.

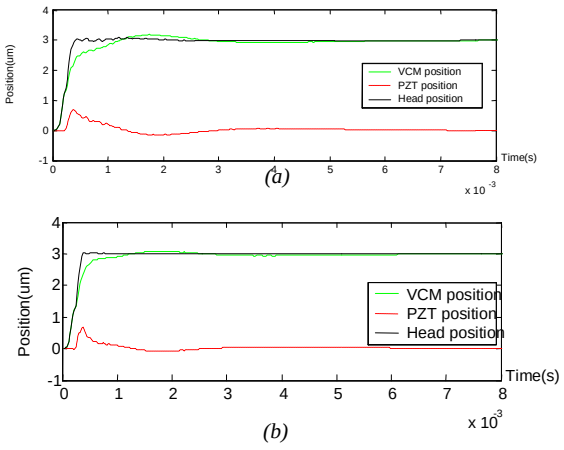

Fig. 10 3-um seeking by two-stage IVA considering PZT saturation: (a) Design I; (b) Design II;

Fig. 10 also indicates how the two actuators contribute to the responses during the short-span seeking. At first, only VCM actuator is activated. When the r/w head approaches *r=1*, PZT actuator is switched on, and the response is such that the PZT actuator first moves to the target track, and then returns to its stroke center to cancel out the movement of the VCM actuator after the head is on track. We can see PZT is within its operation range during the whole short-span seeking.

4. CONCLUSION

This paper has proposed a short seeking control method based on track-following controllers and initial value adjustment for dual-actuator HDDs. IVA improves transient characteristics from the viewpoint of minimizing the performance index function. By incorporating the inter-sampling error and the smoothness of output and control input in the performance index, initial value adjustment of the track-following controllers can achieve desired short seeking performance. To avoid micro-actuator saturation, a two-stage IVA scheme is designed to provide a high-speed movement in the first stage using only VCM loop, and fast and smooth positioning in the second stage using both actuators. Simulations for both 1-track seeking (within PZT stroke limit) and short-span seeking (over PZT stroke limit) are performed. Simulation results confirmed that an excellent short-seeking performance can be achieved without saturating the fine actuator using the proposed method.

REFERENCES

Ding, J., M. Federico and M. Tomizuka, "Short Seeking Control with Minimum Jerk Trajectories for Dual Actuator Hard Disk Drive Systems," *Proc. Amer. Control Conf.*, 2004

Ding, J., M. Tomizuka, and H. Numasato, "Design and robustness analysis of dual stage servo system", *Proc. American Control Conference, Chicago, IL, USA*, June 2000, pp. 2605-2609.

Hernandez, D., S. Park, R. Horowitz, and A. K. Packard, "Dual-stage track-following servo design for hard disk drives," in *Proc. Amer. Control Conf.*, 1999, pp. 4116–4121.

Kobayashi, M. and R. Horowitz, "Track Seek Control for Hard Disk Drive Dual-Stage Servo Systems", *Trans. on Magnetics*, Vol. 37, No. 2, March 2001.

Koganezawa, S., Y. Uematsu, and T. Yamada, "Dual-stage actuator system for magnetic disk drives using a shear mode piezoelectric microactuator," *IEEE Trans. on Magnetics*, vol.35, no.2, Mar. 1999.

Mori, K. *et al.*, "A dual-stage magnetic disk drive actuator using a piezoelectric drive for a high track density," *IEEE Trans. Magn.*, vol. 27, no. 6, pp. 5298–5300, 1991.

Semba, T. *et al.*, "Dual-stage servo controller for HDD using MEMS microactuator," *IEEE Trans. Magn.*, vol.35, no.5, pp.2271–73, 1999.